Indian Journal of Chemistry
Vol. 58B, February 2019, pp. 157-166

Visible light driven photocatalytic degradation of brilliant green dye using graphene oxide/copper oxide binary composite

Rukhsar Banu[a], Nutan Salvi[a], Chetna Ameta[a], Rakshit Ameta[b] & Pinki B Punjabi*[a]

[a] Photochemistry Laboratory, Department of Chemistry, University College of Science,
M. L. Sukhadia University, Udaipur 313 002, India

[b] Department of Chemistry, J. R. N. Rajasthan Vidyapeeth (Deemed to be University), Udaipur 313 001, India

E-mail: pb_punjabi@yahoo.com; rukhs.sonu@gmail.com

Received 16 June 2018

In the present work, photocatalytic degradation of brilliant green has been carried out using graphene oxide/copper oxide (GO/CuO) composite as photocatalyst under visible light. GO/CuO composite has been prepared by hydrothermal method. It has been characterized by XRD, FESEM and FT-IR spectroscopy. The rate of degradation of dye has been monitored spectrophotometrically by measuring absorbance of dye after regular time intervals. The effect of various parameters such as *p*H, concentration of dye, photocatalyst dosage and light intensity on the rate of reaction has been studied. Various parameters like chemical oxygen demand (COD), conductance, *p*H, TDS, salinity and dissolved oxygen (DO) for the reaction mixture before and after photocatalytic degradation have been determined. Reusability of the synthesized catalyst has also been assessed.

Keywords: Graphene oxide/Copper oxide, brilliant green, photocatalyst

Water pollutants discharged from various dyeing and printing industries is one of the most severe ecological threats in the world[1-3]. Most of the dyes released from industries are mutagenic, toxic and teratogenic that can cause serious health problems to humans and livestock[4]. Dyes released into environment can impart color to water and also decrease or stop capacity of water reoxygenation by blocking sunlight thereby increasing BOD value. Therefore, these conditions can prevent or disturb the growth of aquatic plants and animals[5,6].

Organic synthetic dyes have excellent stability, which results in large amounts of wastewater containing dyes being released into the environment. The color of wastewater containing dyes can inhibit photosynthesis of aquatic plants and cause deterioration of water quality. Carcinogenic and toxic effects of some dyes are harmful to human beings and aquatic life[7-9].

In the past several years, many physical techniques have been used to reduce the toxic dye effluents from waste water[10,11]. These techniques are photodegradation, coagulation, flocculation, reverse osmosis, adsorption on the activated carbon, ion exchange method, ultra-filtration and chemical methods like photosensitized oxidation, *etc*., although these methods are fairly effective in removing pollutants, but the main drawback of these techniques is formation of secondary waste products, which cannot be treated again and dumped as such[12,13]. The most recent advances in the field of water treatment have been made in the oxidation of "biologically recalcitrant" organic compounds present in the release of various industries especially of textile sector. These methods decompose the more recalcitrant molecules into biologically degradable molecules or in mineral compounds such as CO_2 and H_2O. These technologies are called Advanced Oxidation Processes (AOPs).

Among various AOPs, photocatalysis has attracted significant attention because of its low-cost, heterogeneous nature, environmental friendliness and sustainability[14,15]. This is a technology that has great potential to control aqueous organic contaminants or pollutants. Most of the photocatalysts are metal oxides (*e.g*., TiO_2, ZnO, *etc*.) and chalcogenides (*e.g*., ZnS, CdS, CdSe, ZnSe, CdTe, *etc*.).

Cupric oxide (CuO), a p-type semiconductor with monoclinic structure. Among the large family of metal oxides, cupric oxide is an interesting multifunctional material due to its promising

applications in magnetic storage, solar energy transformation, electronics, sensors, batteries and catalysis[16]. CuO crystal structure has a narrow band gap due to which it has useful photovoltaic or photocatalytic properties as well as photoconductive functionalities[17].

In last few years, graphene has also attracted the attention of scientific community due to its facile synthesis and various applications as novel hybrid material. Graphene, however, has a major drawback of having low dispersibility in water, causing its surface area to decrease, and therefore, limits its applications. This is due to aggregation that is caused by the strong van der Waals interactions and π–π stacking of the graphene sheets[18]. Therefore, interest has been concentrated on hybridizing graphene oxide (GO) with other materials possessing good water-dispersibility[19]. Graphene oxide contains cluster of reactive oxygen functional groups. This feature makes GO a strong nominee for its use in many applications through chemical functionalization. Graphene oxide is receiving attention because it possesses the similar properties to graphene as well as the special surface structures with the introduced hydroxyl and carboxyl groups for the synthesis of GO-containing nanocomposites[20].

Number of metal oxide/graphene oxide nanocomposites have been synthesized and investigated for photocatalytic degradation of organic dyes. Ji *et al.*[21] have synthesized Ag_2O/GO nanocomposite and investigated degradation of methylene blue under visible light. Rong *et al.*[22] reported removal of methylene blue from aqueous solution by synergetic effects of adsorption and photodegradation using NiO/graphene oxide nanocomposite. Graphene oxide–Fe_2O_3 hybrid material has been reported as highly efficient heterogeneous catalyst for degradation of organic contaminants by Guo *et al.*[23] while Hosseini and Babaei[24] reported graphene oxide/zinc oxide (GO/ZnO) nanocomposite as a superior photocatalyst for degradation of methylene blue analyzing the results by response surface methodology. Stengal *et al.*[25] synthesized TiO_2-graphene oxide nanocomposite as advanced photocatalytic material. This photocatalytic material was prepared by thermal hydrolysis of suspension of graphene oxide nanosheets and titania peroxo-complex. Wang *et al.*[26] carried out *in situ* synthesis of Cu_2O in the regenerated chitin/graphene oxide composite film and used it as photocatalyst under sunlight.

In the present work, we have prepared graphene oxide/copper oxide composite by hydrothermal method. The photocatalytic activity was tested by degrading a dye, Brilliant green (BG) under visible light irradiation. Properties of the prepared samples were characterized, and effects of parameters of photocatalytic reacting systems on removal efficiencies of BG were also studied and discussed. BG ($C_{27}H_{34}N_2O_4S$, MW 482.64 g/mol, λ_{max} = 625 nm), a triarylmethane (TAM) dye, has been used as colorants in industry and as antimicrobial agents[27]. BG is widely used in modern textile industries. Brilliant green is also used in large scale of staining and biological applications such as skin staining, large intestine staining, coloring of fibers, inks, printed circuit boards. BG causes some degree of carcinogenicity, hypersensitivity reactions, microbial and fish toxicity[28].

Experimental Section

Materials

Graphite flakes (Merck), Potassium permanganate (Thomas Baker), Sodium nitrate (Rankem), copper nitrate trihydrate (Fisher Scientific), *p*H meter (Systronics Model 335), Solarimeter (CEL Model SM 201), spectrophotometer (Systronics Model 106), Brilliant green (Himedia) and hydrogen peroxide (CDH, 30% w/v) were used as received commercially. All the chemicals used were of analytical grade.

Synthesis of GO

GO was synthesized using natural graphite by the modified Hummers method[29]. In a typical synthesis, 2 g of graphite powder and 2 g of sodium nitrate was added into 90 mL of 98% H_2SO_4 under continuous stirring for 4 h at 0°C in an ice bath. Then 12 g of $KMnO_4$ was added slowly to the above solution keeping the reaction temperature lower than 15°C. The reaction mixture is diluted with 200 mL of distilled water under stirring for 2 h. The ice bath was then removed, and the mixture was stirred at 35°C for 2 h. This mixture was then refluxed at 98°C for 10-15 min. After 10 min, the temperature was changed to 30°C, which gives brown colored solution. Again after 10 min, the temperature was changed to 25°C, and maintained it for 2 h. The solution is finally treated with 40 mL H_2O_2 to remove excess $KMnO_4$, which resulted in bright yellow reaction mixture. 200 mL of water was added to the reaction mixture

and stirred for 1 h. Now the reaction mixture was kept for 3-4 h under ambient conditions (without stirring) so that the graphene oxide particles settle at the bottom. The supernatant water is poured and the graphene oxide is washed repeatedly with 10% HCl and with deionized water to give gel like required compound. Further, it was vacuum dried at 60°C for 6-7 h to obtain graphene oxide powder.

Synthesis of GO/CuO composite

CuO nanoparticles were prepared by thermal decomposition of copper nitrate trihydrate ($Cu(NO_3)_2.3H_2O$) at 350°C for 2 h. The black particles were dispersed in 100 mL of 1% acetic acid, where CuO changed into copper cations. To this, 1 g of graphene oxide was added. This solution was irradiated with microwave radiation for 8 min. In this solution 1 mL of NaOH was added drop wise until the solution attained *p*H 10. The GO/CuO nanocomposite in the form of residue was obtained. The contents were heated at 80°C for 5 h and then filtered and washed with excess of water and dried in a vacuum oven at 60°C for overnight.

Results and Discussion

Field emission scanning electron microscopy (FESEM)

The size and surface morphology was observed by the field emission scanning electron microscope. It was recorded on the JEOL JSM-6390LV SEM fitted with secondary electron detector. FESEM study of CuO nanoparticles exhibit triangular shaped petals was almost uniform and homogenous and these petals united to form flower like structure of CuO nanoparticles[30]. FESEM images of GO showed lamellar sheet like structure of graphene oxide with multilayers[31].

FESEM images of synthesized GO/CuO composite are shown in Figure 1. As shown in Figure 1a, it is clear that the diameter size of nanoflower is about 6 μm. This nanoflower like structure represents CuO nanoparticles, which is formed by rod shaped petals with a typical thickness around 23 nm and

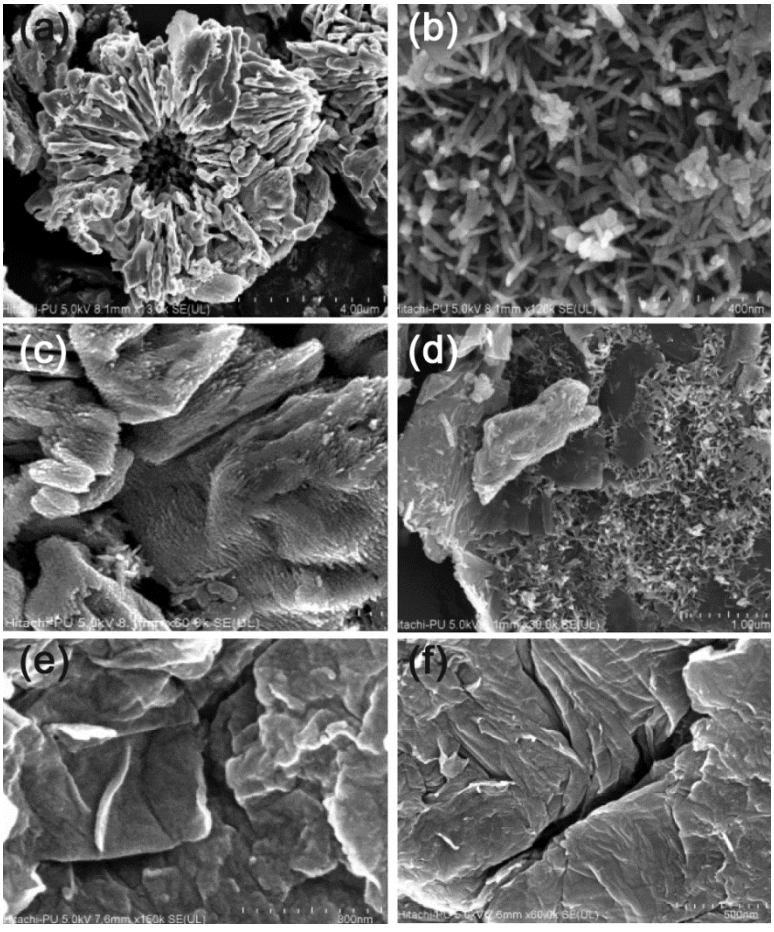

Figure 1 — FESEM images of GO/CuO composite

length of rod is around 85 nm (Figure 1b). In Figure 1c lamellar sheets indicate the presence of GO layers. The rod shaped petals of CuO nanoparticles are well decorated on the surface of lamellar graphene oxide sheets is clearly shown in Figure 1c and Figure 1d. It is further demonstrated that an adequate interfacial contact is developed between the CuO nanoparticles and GO sheets. This type of interfacial contact of metal particle and GO sheet is favorable for effective charge transfer between CuO nanoparticles and GO sheets. Synthesized GO shows lamellar sheet like structure which is clearly shown in Figure 1e and Figure 1f.

Fourier transform infrared spectroscopy (FTIR)

FT-IR spectroscopy is an important technique to characterize the presence of different functional groups in graphene oxide and its composites. Figure 2a shows the FT-IR spectrum of pure graphene oxide. The major peaks are at about 3850, 3739, 3127, 2865, 2930, 2317, 1734, 1635, 1405, 1228, 1058, 858 and 664 cm^{-1}, *etc*. The absorbed water in GO is shown by broad peaks at 2885, 3127, 3739 and 3850 cm^{-1}, contributed by the O-H group of stretching vibrations of carbonyl, alcohol and absorbed water molecules. Absorption band at 1635 cm^{-1} corresponding to the C=C bonds (unoxidized sp^2 C-C

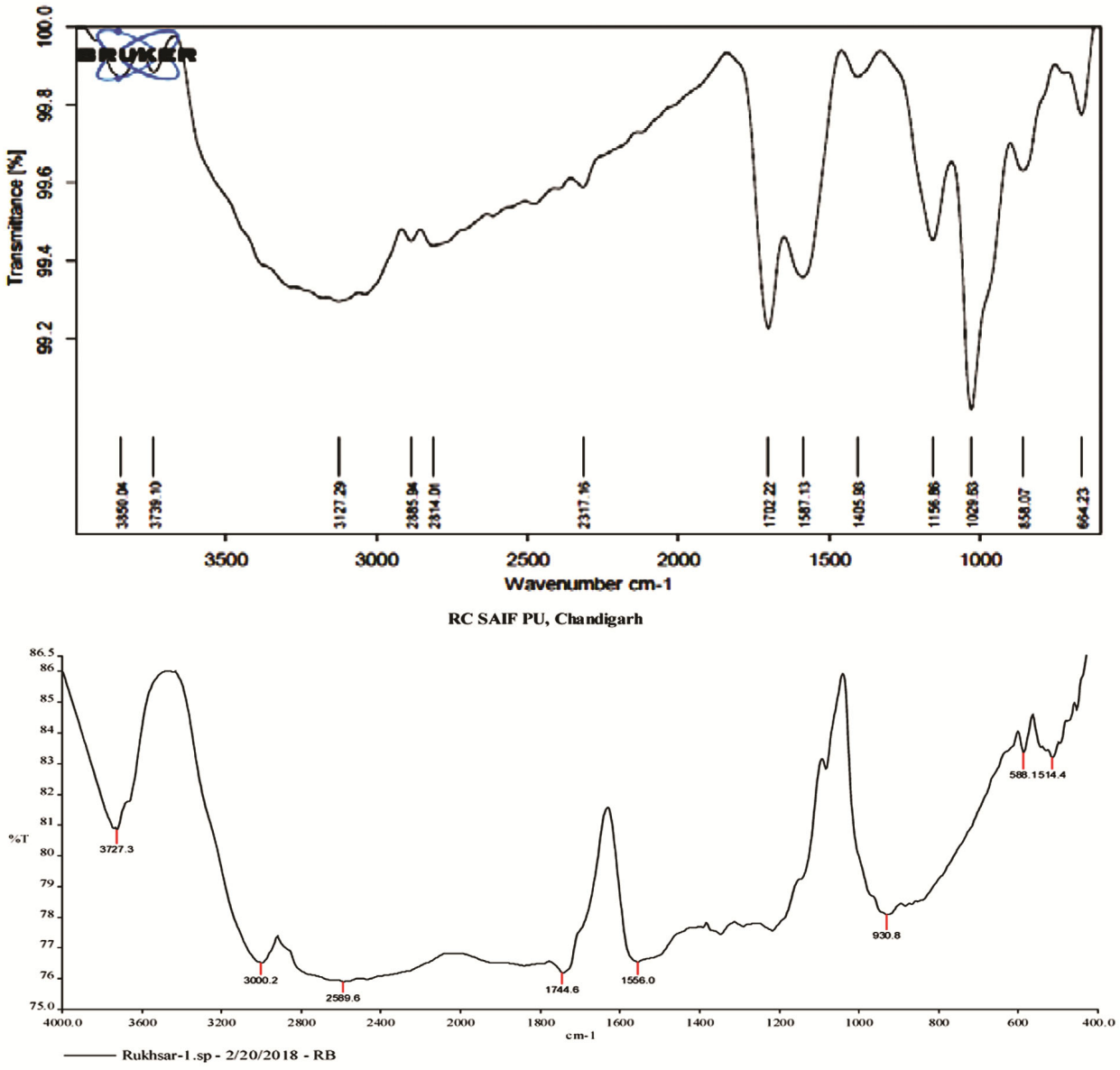

Figure 2 — (a) FT-IR spectra of GO; (b) FT-IR spectra of GO/CuO composite

bonds) and 1228 cm^{-1} assigned to C–O stretching vibrations of phenolic C–OH. Two intense peaks appeared at 2865 and 2930 cm^{-1} that represents symmetric and asymmetric $=CH_2$ vibrations of graphene, respectively[32]. The IR spectrum of GO shows the strong C=O stretching band of –COOH group at 1734 cm^{-1}. IR peaks of 1405 and 1058 cm^{-1} shows C-OH vibrations and C-O stretching of epoxy groups, respectively.

Figure 2b shows nanocomposite of GO with CuO in the range of 4000 to 400 cm^{-1}, which confirms the presence of different oxygen functional groups such as hydroxyl, carboxyl and epoxy on the GO sheets and thus confirms the successful synthesis of the GO. In the FTIR spectra of GO, the broad and the most intense peak between 3000-3727 cm^{-1} can be assigned to the superimposed stretching vibrations of O–H group of the carbonyl, alcoholic and the absorbed water molecules. The other characteristic GO peaks are observed at 930 cm^{-1} assigned to C–O stretching vibrations of epoxy groups, 1744 cm^{-1} assigned to C=O stretching vibrations of COOH groups whereas the peak at 1556 cm^{-1} can be assigned to the H–O–H bending vibrations or adsorbed water molecules or to the skeletal vibrations of unoxidized C–C bonding. Absorption band of peak at 1220 cm^{-1} is assigned to C–O stretching vibrations of phenolic C–OH. All the peaks related to the oxygen-containing functional groups indicate the oxidation of graphite. The formation of CuO phase is characterized and confirmed by the presence of strong and sharp IR peaks at 588, and 514 cm^{-1} that can be assigned to the stretching of Cu–O group. Hence, the FTIR study confirms the synthesis of CuO/GO composites.

X-ray diffraction (XRD)

The crystallinity of GO/CuO powder was determined by X-ray diffraction (XRD) using XPERT-PRO diffractometer with Cu K_α radiation. The accelerating voltage and the applied current were 35 kV and 20 mA, respectively. It shows the diffraction peak at 2θ=10.47°, which is mainly due to the oxidation of graphite. The diffraction peak of pure graphite is found around 26°, corresponding to the highly organized layer structure with an interlayer distance of 0.34 nm is shown as inset in Figure 3a. Diffraction peak at 2θ=42.26°, indicates a short range order in stacked graphene layers. The diffraction patterns were processed using Fityk software.

The XRD pattern revealed the orientation and crystalline nature of material. Figure 3b shows the X-ray diffraction pattern of the prepared sample. The XRD peak position was consistent with the graphene oxide/copper oxide composite. The sharp peaks with

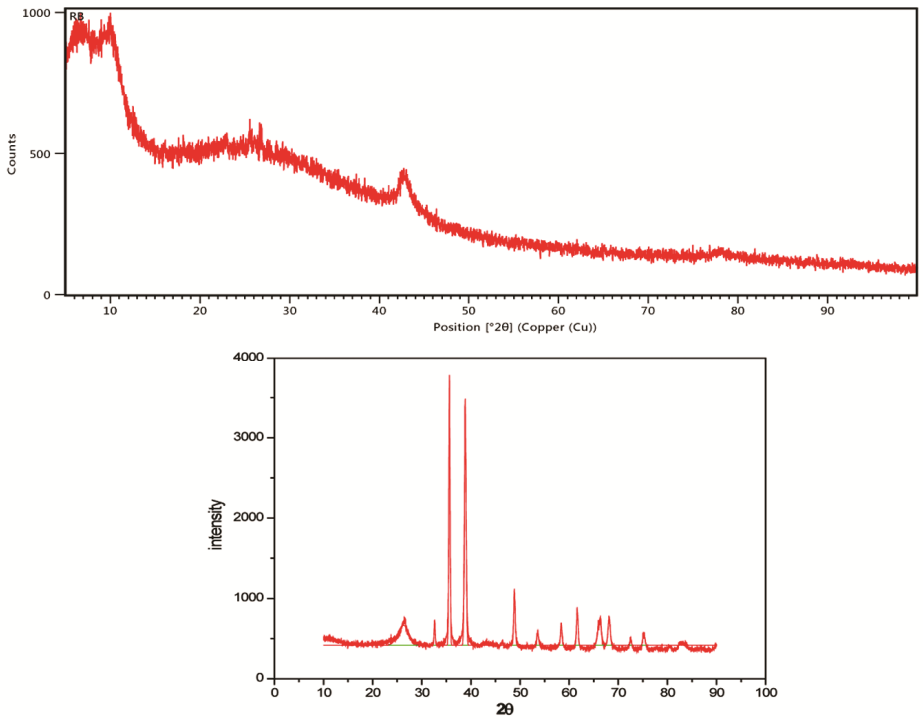

Figure 3 — (a) XRD of GO; (b) XRD of GO/CuO

high intensity indicated the crystalline nature. The diffraction peak at 26.26 nm shows the presence of pure graphite. The particle size of diffraction peak is found to be 4 nm. The diffraction peak at 12° which shows complete oxidation of graphite, could not be seen, which means that after synthesis of GO/CuO composite, the product is not in its completely oxidized form. The diffraction peaks observed at 32.62°, 35.40°, 38.62°, 48.65°, 53.6°, 58.39°, 61.65°, 66.2°, 68.14°, 72.5°, 75.21° and their particle sizes are 36, 32, 24, 27, 25, 28, 29, 13, 22, 38 and 25 nm, respectively of the monoclinic structure of CuO (JCPDS:80-1916). Peaks of impurities not detected, indicating that the CuO nanoparticles are pure and highly crystalline. The above observations revealed that the prepared composite is nano sized.

Photocatalytic procedure

The photocatalytic activity of the catalyst was evaluated by determining the rate of degradation of brilliant green (BG). A stock solution of dye (1.0×10^{-3} M) was prepared by dissolving dye (0.0483 g) in 100 mL of doubly distilled water. The stock solution was further diluted to 1.0×10^{-5} M. 0.07 g of photocatalyst was added to it and *p*H was adjusted to 7.5. *p*H of the dye solution was measured by a digital *p*H meter and the desired *p*H of the dye solution was adjusted by the addition of standard 0.1 N sulphuric acid and 0.1 N sodium hydroxide solutions. The reaction mixture was exposed to a 200 W tungsten lamp, and 2.5 mL aliquot was taken out after every 5 min. Absorbance (A) was measured at λ_{max} = 625 nm. A water filter was used to cut off thermal radiations. The intensity of light was varied by changing the distance between the light source and reaction mixture, and it was measured by Solarimeter. The absorbance of the solution at various time intervals was measured with the help of spectrophotometer.

It was observed that the absorbance of the reaction mixture decreases with increasing the time of exposure, which indicates that the concentration of brilliant green dye decreases with increase in time. The degradation efficiency (φ) was calculated by following expression:

$$\varphi = 100\frac{A-A_0}{A_0} \quad \ldots (1)$$

Here A_0 is initial absorbance, and A is absorbance after degradation of dye at particular time t. A plot of 2 + log A *versus* time was linear following pseudo-first order kinetics.

The rate constant, k was calculated by using the expression:

$$k = 2.303 \times \text{slope} \quad \ldots (2)$$

Typical run for the degradation of brilliant green under optimum conditions are reported in Figure 4 and Table I.

[Brilliant green] = 2.50×10^{-5} M, *p*H = 7.5, GO/CuO composite = 0.070 g, Light intensity = 50.0 mWcm^{-2}

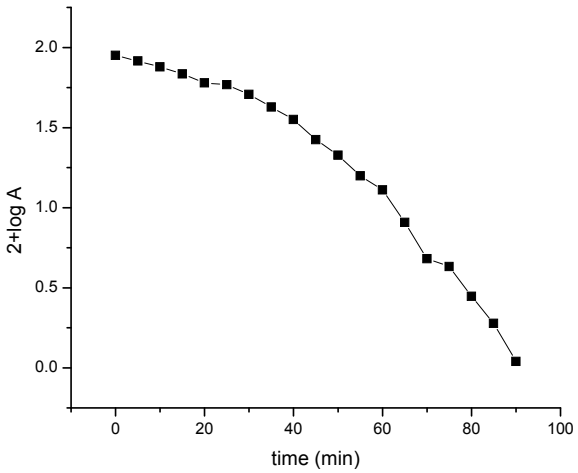

Figure 4 — Typical run for photocatalytic degradation of Brilliant green

Table I — Typical run for photocatalytic degradation of brilliant green

Time (min)	Absorbance (A)	2 + log A
0	0.894	1.9513
5	0.825	1.9164
10	0.758	1.8796
15	0.685	1.8356
20	0.603	1.7803
25	0.587	1.7686
30	0.510	1.7075
35	0.425	1.6283
40	0.356	1.5514
45	0.266	1.4248
50	0.213	1.3283
55	0.158	1.1986
60	0.129	1.1105
65	0.081	0.9084
70	0.048	0.6812
75	0.043	0.6334
80	0.023	0.4471
85	0.019	0.2787
90	0.011	0.0413
Rate constant k, (s^{-1})	8.51×10^{-5}	
Ψ, % (1st run)		98.76
(2nd run)		96.50

Effect of parameters

Effect of *p*H

The rate of degradation has been investigated in the *p*H range 5-9 keeping other parameters identical. The results are summarized in Figure 5. It was observed that with an increase in *p*H, the rate of reaction increases. After attaining the maximum value at *p*H 7.5, the rate decreases with a further increase in *p*H. The increase in rate of photocatalytic degradation may be due to the more availability of hydroxyl ions at higher *p*H, which remain adsorbed on the GO/CuO catalyst surface making it negatively charged. Therefore, a large number of cationic dye molecules approach the GO/CuO catalyst surface due to coulombic attraction between oppositely charged dye molecules and GO/CuO catalyst surface. On the surface, these dye molecules undergo photocatalytic oxidation by $^{\bullet}OH$ radicals. After a certain value of *p*H (7.5), a further increase in *p*H of medium, decreases the rate of photodegradation. It may be due to the fact that the dye does not remain in its cationic form due to greater concentration of OH^{-} ions, therefore, coulombic attraction between BG and GO/CuO surface decreases. As a result, the reaction rate decreases. The participation of various types of radicals has been confirmed by using 2-propanol (scavenger) as the rate of reaction was drastically reduced in its presence.

Effect of BG concentration

The effect of variation of concentration of brilliant green on its degradation rate has been observed in the range from 0.5×10^{-5} to 4.5×10^{-5} M keeping all other parameters same. It has been observed that the rate of degradation increases with increasing concentration of dye up to 2.5×10^{-5} M. Further increase in concentration beyond this limit results in a decrease in degradation rate. This may be explained on the basis that on increasing the concentration of dye, the reaction rate increases as more molecules of dyes are available for degradation but a further increase in concentration beyond this limit dye molecules act as internal filter which does not permit sufficient amount of light to reach the surface of the photocatalyst thus, decreasing the rate of photocatalytic degradation of brilliant green (Figure 6).

The effect of photocatalyst dosage

The effect of variation of the dosage of photocatalyst on the rate of dye degradation has been studied in the range from 0.02 to 0.10 g /50 mL reaction mixture. It has been observed that with an increase in the dosage of photocatalyst, the rate of degradation increases to a certain amount of catalyst *i.e*. 0.07 g. Beyond this limit, the rate of reaction was decreased on increasing the concentration of photocatalyst. This behavior may be explained by the fact that with an increase in the dosage of photocatalyst, the exposed surface area of photocatalyst will increase. Hence, the rise in the rate of reaction has been observed, but with further increase in the dosage of photocatalyst after 0.07 g, it would also increase the number of copper ions and then there is a possibility of short circuiting of cuprous(I) and cupric (II) ions[33-35]. As a result, fewer hydroxyl radicals are formed and reaction rate is retarded (Figure 7).

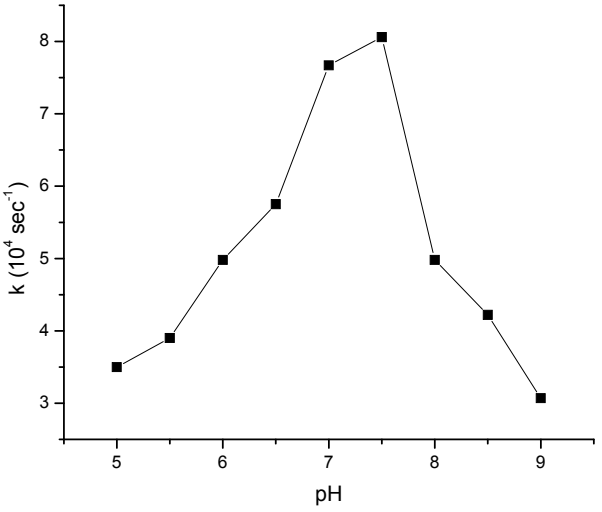

Figure 5 — Effect of *p*H on photocatalytic degradation of brilliant green

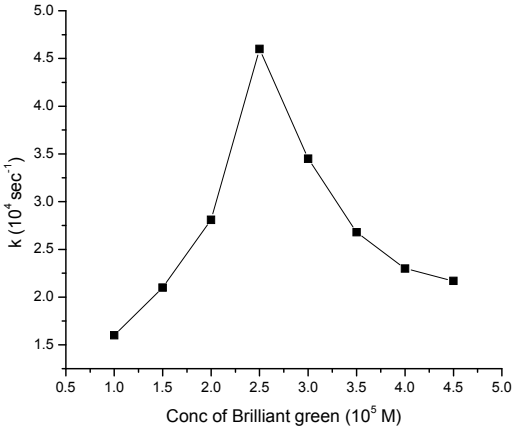

Figure 6 — Effect of BG concentration on its photocatalytic degradation

The effect of light intensity

The effect of light intensity on the rate of dye degradation was also studied by varying the intensity of light from 10.0 to 70.0 mWcm^{-2}. From Figure 8, it is clear that with increasing light intensity, the rate of reaction increases and maximum rates were found at 50.0 mW cm^{-2}. It may be explained on the basis that as the light intensity was increased, the number of photons striking per unit area also increased, resulting in higher rate of degradation. Further increase in the light intensity may start some thermal side reactions, decreasing the rate of reaction.

Reusability of photocatalyst

The reusability of the photocatalyst was assessed by recycling GO/CuO composite three times, and the rate of degradation of BG was monitored each time.

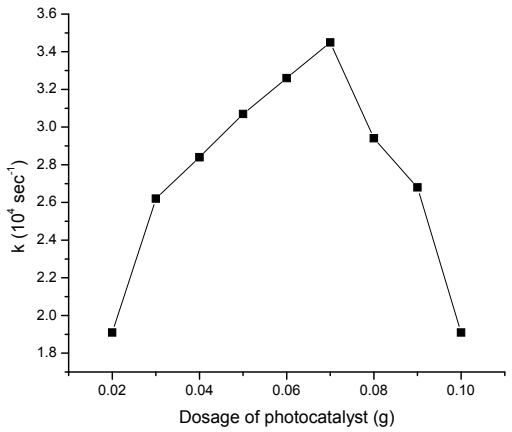

Figure 7 — Effect of dosage of catalyst on photocatalytic degradation of brilliant green

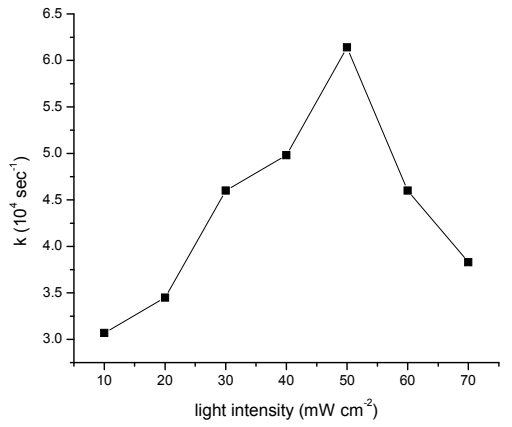

Figure 8 — Effect of light intensity on photocatalytic degradation of brilliant green

The removal efficiency of BG was 98.76% in the first run, 96.5% in the second run and only 20% in the third run for 90 min exposure under visible light irradiation. The slight decrease can be attributed to the loss of photocatalyst between two runs and some refractory intermediates adsorbed on their surface which are difficult to be destroyed[36].

Mechanism

The electron-hole generated in photocatalyst can produce various types of radicals like hydroperoxide, hydroxyl radicals and superoxide anion radical (O2$^{-\bullet}$), which can decompose dye to CO_2, H_2O and inorganic species. In a photocatalytic system, a reaction takes place at the surface of the catalyst. Photocatalytic decomposition of BG was driven by the participation of $^{\bullet}OH$ and e^-, and also by the contribution of h^+, $HO_2^{\bullet}$ and $O_2^{-\bullet}$. When a photocatalyst is exposed by a light greater than its band gap energy, the valance band (VB) electrons (e^-) of the photocatalyst are excited to the conduction band (CB), creating holes (h^+) in the VB. Electron-hole pairs diffuse out to the surface of the photocatalyst and participate in a chemical reaction with the electron donor and acceptor. These free electrons and holes transform the surrounding oxygen or water molecules into hydroperoxide radical, superoxide anion radical ($O_2^{-\bullet}$) and specially hydroxyl radicals. These free radicals are then used to decompose the organic pollutant into carbon dioxide and water.

A highly efficient visible light photocatalysis should have high quantum efficiency resulting from low recombination of the photogenerated electron-hole pair and a wide visible light response range because of the narrow band gap. With the presence of excellent electron-mobility of GO anchored to a CuO photocatalyst, the charge transport rate could be increased, therefore, inhibiting the charge recombination and promoting the photocatalytic activity. The presence of GO could reduce the band gap which promotes an excellent photocatalytic activity.

$$CuO + hv \longrightarrow CuO(h^+) + CuO(e^-) \quad (3)$$

$$CuO(e^-) \longrightarrow CuO + GO(e^-) \quad (4)$$

$$e^- + O_2 \longrightarrow O_2^{-\bullet} \quad (5)$$

$$h^+ + {}^-OH \longrightarrow {}^{\bullet}OH \quad (6)$$

$$O_2^{\bullet -} + H^+ \longrightarrow HO_2^{\bullet} \quad (7)$$

$$BG + O_2^{\bullet -} + HO_2^{\bullet} + {}^{\bullet}OH \longrightarrow \text{Mineralized products Like } CO_2, H_2O, \text{inorganic ions etc.} \quad (8)$$

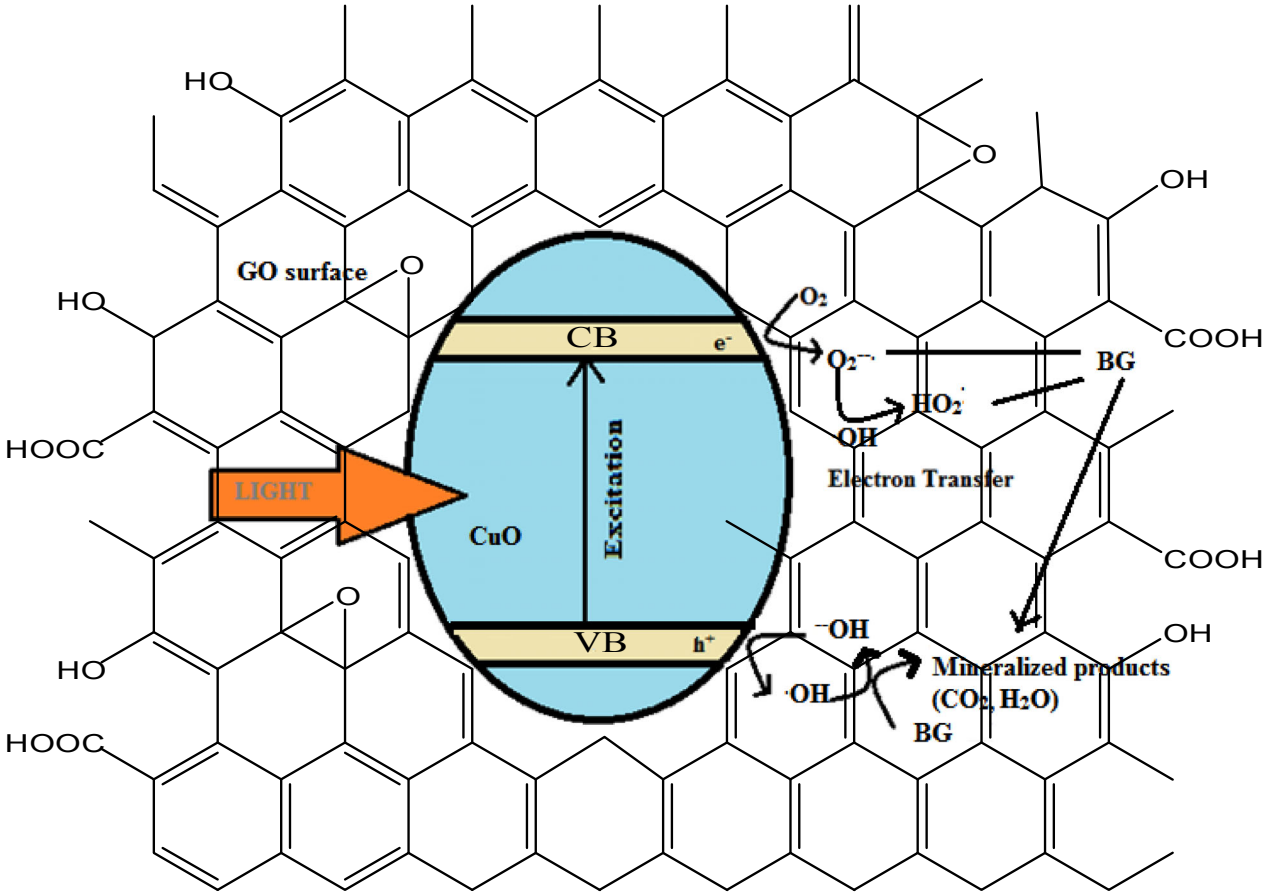

Figure 9 — Mechanism of GO/CuO

Due to the narrow band gap energy (2.05 eV), CuO can be excited by visible light illumination. Thus, when the Xenon lamp irradiated the GO/CuO composite, photogenerated electrons in the conduction band (CB) and holes in the valence band (VB) of CuO were generated, respectively. Afterwards, electrons in the CB of CuO would easily transfer to the surface of GO. Therefore, the separation efficiency of photogenerated charge carriers was greatly improved. On one hand, electrons on the surface of GO could reduce absorbed compounds (such as O_2, H^+, *etc*). On the other hand, photoinduced holes in the VB of CuO could react with the contaminants or OH to form $^{\bullet}OH$ radicals and consequently degrade brilliant green. The participation of various types of radicals have been confirmed by using butylated hydroxytoluene (BHT) scavenger as the rate of reaction was drastically reduced in its presence. A diagrammatic presentation of photocatalytic degradation of BG over GO/CuO composite is given in Figure 9.

Conclusions

Photocatalytic reactions are the most effective methods for the treatment of waste water. In the dark, the rate of reaction is very slow, whereas semiconductor based photocatalytic degradation in presence of visible light offers a good choice for treatment of waste water. In the present work, graphene oxide/copper oxide has been used as heterogeneous photocatalyst to degrade brilliant green dye successfully with 98% efficiency. The participation of $HO^{\bullet}$, $HO_2^{\bullet}$ and $O_2^{-\bullet}$ radicals as active oxidizing species was confirmed by carrying out the reaction in the presence of radical scavenger BHT, where the rate of reaction was drastically retarded. Results indicated that simultaneous utilization of all the parameters under optimal conditions increases the rate of degradation of dye. The dye quickly lost its color, indicating that the dissolved dye has been oxidized. It has also been observed that catalyst can be reused twice with almost same efficiency.

Acknowledgements

One of the authors, Rukhsar Banu, is thankful to University Grants Commission, New Delhi for the award of MANF, JRF. The authors are also thankful to SAIF, CIL Laboratories (Chandigarh) for providing FT-IR, FESEM and XRD data. Thanks are also due to Head, Department of Chemistry, M. L. Sukhadia University, Udaipur for providing laboratory facilities.

References

1 Pokhrel D & Viraraghavan T, *Science of the Total Environment*, 333 (2004) 37.
2 Du X, Ding Y & Xiang X, *Energy Environ Focus*, 4 (2015) 307.
3 Cho H, Liu G, Zhang Z, Qiao P, Shan Z & Hwang W, *Sci Adv Mater*, 7 (2015) 2623.
4 Mekkawy H A, Ali M O & El-Zawahry A M, *Toxicol Lett*, 95 (1998) 155.
5 Song Y L, Tai J & Bai B, *Water Air Soil Pollut*, 213 (2010) 311.
6 Wang S, *Dyes Pigm*, 76 (2008) 714.
7 Umar A, Akhtar M, Al-Hajry A, Al-Assiri M, Dar G & Islam M, *Chem Eng J*, 262 (2015) 588.
8 Ameena S, Akhtarb M, Kim Y & Shina H, *Appl Catal B*, 103 (2011) 136.
9 Wang Y & Chu W, *J Hazard Mater*, 186 (2011) 1455.
10 Li X, Liu G & Zhao J, *New J Chem*, 23 (1999) 1193.
11 Serpone N, *Res Chem Intermediat*, 20 (1994) 953.
12 Ferreira C, Domenech S & Lacaze P, *J Appl Electrochem*, 31 (2001) 49.
13 Saquib M & Muneer M, *Dyes Pigm*, 56 (2003) 37.
14 Gómez-Pastora J, Dominguez S, Bringas E, Rivero M J, Ortiz I & Dionysiou D D, *Chem Eng J*, 310 (2017) 407.
15 Bagheri H, Afkhami A & Noroozi A, *Anal Bioanal Chem Res*, 3 (2016) 1.
16 Applerot G, Lellouche J, Lipovsky A, Nitzan Y, Lubart R, Gedanken A & Banin E, *Small*, 8 (2012) 3326.
17 Ren G, Hu D, Cheng E W C, Vargas-Reus M A, Reip P & Allaker R P, *Int J Antimicrob Agents*, 33 (2009) 587.
18 Huang X, Yin Z, Wu S, Qi X, He Q, Zhang Q, Yan Q, Boey F & Zhang H, *Small*, 7 (2011) 1876.
19 Liu J, Liu G & Liu W, *Chem Eng J*, 257 (2014) 299.
20 Dreyer D R, Park S, Bielawski C W & Ruoff R S, *Chem Soc Rev*, 39 (2010) 228.
21 Ji Z, Shen X, Yang J, Xu Y, Zhu G & Chen K, *Eur J Inorg Chem*, 36 (2013) 6119.
22 Rong X, Qiu F, Zhang C, Fu L, Wang Y & Yang D, *Powder Technol*, 275 (2015) 322.
23 Guo S, Zhang G, Guo Y & Yu J C, *Carbon*, 60 (2013) 437.
24 Hosseini S A & Babaei S, *J Braz Chem Soc*, 28 (2017) 299.
25 Stengl V, Bakardjieva S, Grygar T M, Bludska J & Kormunda M, *Chem Cent J*, 7 (2013) 1.
26 Wang Y, Pei Y, Xiong W, Liu T, Li J, Liu S & Li B, *Int J Biol Macromol*, 81 (2015) 477.
27 Duxbury D F, *Chem Rev*, 93 (1993) 381.
28 Vachalkova A, Novotny L & Blesova M, *Neoplasma*, 43 (1996) 113.
29 Paulchamy B, Arthi G & Lignesh B D, *J Nanomed Nanotechnol*, 6 (2015) 253.
30 'Synthesis and Characterization of Cupric Oxide Thin Films by Sol-Gel Method', IEEE-ICSE2014 Proc. 2014, Kuala Lumpur, Malaysia,
31 Mishra A K & Ramaprabhu S, *J Phys Chem C*, 115 (2011) 14006.
32 Jiang N, Xiu Z, Xie Z, Li H, Zhao G, Wang W, Wu Y & Hao X, *New J Chem*, 38 (2014) 4312.
33 Klauson D, Preis S, Portjanskaja E, Kachina A, Krichevskayz M & Kallas J, *Environ Technol*, 26 (2005) 653.
34 Munoz M J L, Aguado J & Ruperez B, *Res Chem Intermed*, 33 (2007) 377.
35 Kalal S, Chauhan N P S, Ameta N, Ameta R, Kumar S & Punjabi P B, *Korean J Chem Eng*, 31 (2014) 2183.
36 Meng X, Jiang L, Wang W & Zhang Z, *Int J Photoenergy*, Vol. 2015, Article ID 747024, 9 pages (2015).